The Long Noncoding MALAT-1 RNA Indicates a Poor Prognosis in Non-small Cell Lung Cancer and Induces Migration and Tumor Growth

Lars Henning Schmidt, MD, Tilmann Spieker, MD,† Steffen Koschmieder, MD,* Julia Humberg,* Dominik Jungen, PhD,* Etmar Bulk, PhD,* Antje Hascher, PhD,* Danielle Wittmer,* Alessandro Marra, MD,‡ Ludger Hillejan, MD,‡ Karsten Wiebe, MD,§ Wolfgang E. Berdel, MD,* Rainer Wiewrodt, MD,* and Carsten Muller-Tidow, MD**

Introduction: The functions of large noncoding RNAs (ncRNAs) have remained elusive in many cases. Metastasis-Associated-in-Lung-Adenocarcinoma-Transcript-1 (MALAT-1) is an ncRNA that is highly expressed in several tumor types.

Methods: Overexpression and RNA interference (RNAi) approaches were used for the analysis of the biological functions of MALAT-1 RNA. Tumor growth was studied in nude mice. For prognostic analysis, MALAT-1 RNA was detected on paraffin-embedded non-small cell lung cancer (NSCLC) tissue probes (n = 352) using in situ hybridization.

Results: MALAT-1 was highly expressed in several human NSCLC cell lines. MALAT-1 expression was regulated by an endogenous negative feedback loop. In A549 NSCLCs, RNAi-mediated suppression of MALAT-1 RNA suppressed migration and clonogenic growth. Forced expression of MALAT-1 in NIH 3T3 cells significantly increased migration. Upon injection into nude mice, NSCLC xenografts with decreased MALAT-1 expression were impaired in tumor formation and growth. In situ hybridization on paraffin-embedded lung cancer tissue probes revealed that high MALAT-1 RNA expression in squamous cell carcinoma of the lung was associated with a poor prognosis. On genetic level, MALAT-1 displays the strongest association with genes involved in cancer like cellular growth, movement, proliferation, signaling, and immune regulation.

Conclusions: These data indicate that MALAT-1 expression levels are associated with patient survival and identify tumor-promoting functions of MALAT-1.

*Department of Medicine A, Hematology, Oncology and Pulmonary Medicine, University Hospital Muenster, Muenster, Germany; †Institute of Pathology, University Hospital Muenster, Muenster, Germany; ‡Department of Thoracic Surgery, Niels-Stensen-Kliniken, Ostercappeln, Germany; and §Department of Thoracic Surgery, University Hospital Muenster, Muenster, Germany.

Address for correspondence: Rainer Wiewrodt, MD, PhD, Department of Medicine A, Westfaelische Wilhelms University, University Hospital, Albert-Schweitzer-Campus 1, Building A1, 48149 Münster, Germany. E-mail: rainer.wiewrodt@ukmuenster.de

Disclosure: The authors declare no conflicts of interest.

The last two authors contributed equally.

ISSN: 1556-0864/11/0612-1984

Key Words: MALAT-1, NSCLC, Tumor biology, RNA interference.

(*J Thorac Oncol.* 2011;6: 1984–1992)

Non-small cell lung cancer (NSCLC) accounts for a large number of cancer-related deaths.[1] Less than 20% of patients diagnosed with NSCLC survive more than 5 years.[2] Poor prognosis of early stage NSCLC is crucially linked to the onset of tumor metastasis after initial surgery.[3] The biological mechanism of metastasis is based on the ability of tumor cells to both enter and leave the vasculature, to settle at peripheral organs, and to develop secondary tumors.[4] This complex multistep process is driven by the expression of specific gene products and genetic mutations.[5–7]

A focus of current research is the analysis of the role of noncoding RNAs (ncRNAs) in cancer development. Within the human genome, a vast variety of nuclear and cytosolic ncRNAs exist, including miRNAs (~22 nt) and piRNAs (18–30 nt), short translational-regulatory RNAs (100–200 nt), and much longer ncRNAs (up to 10,000 nt),[8] all lacking protein-coding capacity.[9,10] Although ncRNAs are abundant, only few ncRNAs have assigned specific functions.[11] Transcriptome analyses identified alterations in ncRNA to occur in various malignancies.[12,13] So far, the function of miRNAs as key components of the RNA interference (RNAi) pathway, their role as tumor suppressors, and their impact on cancerogenesis have been demonstrated.[14,15] Nevertheless, little is known about so-called longer ncRNAs (>1 kb) and their impact on cancerogenesis regulatory processes.[13] Similar to mRNAs, long ncRNAs are also transcribed by RNA polymerase II. Because they lack used open reading frames, they are supposed either to function as genetic regulators or to modulate chromatin, depending on their localization to the nucleus.[16]

Among mammals, metastasis-associated lung adenocarcinoma transcript 1 (MALAT-1) is an evolutionarily highly conserved, long noncoding 8.7-kb transcript. We identified MALAT-1 by subtractive hybridization as an overexpressed transcript in early-stage metastasizing NSCLC.[17] MALAT-1 transcript is located on chromosome 11q13,

known for its strong impact on tumor development and metastasis.[18,19] Because MALAT-1 lacks open reading frames of significant length and in vitro translation of MALAT-1 did not result in protein expression, a regulatory or a controlling function of MALAT-1 is assumed.[17] Besides its overexpression in various human carcinomas,[20] MALAT-1 can also be found in normal human and mouse tissues.[16,17] Recently, MALAT-1 was also reported to be overexpressed in placenta previa and supposed to regulate trophoblast invasion.[21]

Intracellularly, MALAT-1 is specifically retained in nuclear speckles,[16] associated with the modification or storage of the premRNA processing machinery[22] and thus with potential impact on gene regulation.[11] 3′ end processing of MALAT-1 yields a 61-nt RNA, exclusively localized to the cytoplasm with a relatively short half-life (mascRNA, MALAT-1-associated small cytoplasmic RNA) and a stable nuclear retained ncRNA. Although mascRNA folds similar to a tRNA cloverleaf secondary structure, it is recognized by the tRNA processing machinery but not aminoacylated. Because of tRNA mimicry, mascRNA is supposed to take part in MALAT-1 gene regulation.[11]

It was the aim of the underlying study to investigate the biological functions of MALAT-1 in lung cancer. Our results suggest that MALAT-1 transcript induces migration in NSCLCs and stimulates tumor growth and invasion in vivo. In addition, we identify MALAT-1 as a prognostic marker in squamous cell carcinoma of the lung.

MATERIALS AND METHODS

Cell Culture

A549 lung cancer[23] and plat-E cells[24] were cultured in Dulbecco's modified Eagle's medium (DMEM; Invitrogen GmbH, Karlsruhe, Germany) at 37°C, high humidity, and 5% CO_2. Medium was supplemented with 10% fetal calf serum, 100 U/mL penicillin, and 100 μg/mL streptomycin. The human lung squamous carcinoma cell line HTB-58 was cultured in Eagle modified essential medium supplemented with 0.1 mM nonessential amino acids, 1 mM sodium pyruvate, 2 mM L-glutamine, 10% heat-inactivated fetal bovine serum, 100 U/mL penicillin, and 100 μg/mL streptomycin. Mouse NIH 3T3 fibroblasts were maintained in DMEM medium enriched with 10% fetal bovine serum, 2 mM L-Glutamine, 100 U/mL penicillin, and 100 μg/mL streptomycin. Cell viability was evaluated by trypan blue exclusion assay.

Cloning and Transfection of a MALAT-1 Expression Vector

Long distance polymerase chain reaction (PCR) (Expand Long Range dNTPack, Roche Diagnostics GmbH, Mannheim, Germany) was used to amplify MALAT-1 DNA from a BAC clone (RPCIB753D15472Q; ImaGenes GmbH, Berlin, Germany). PCR primers contained *att*B-sites and the PCR product was recombined (BP clonase, Gateway technology, Invitrogen GmbH) into pDONR222 vector.[25] Finally, MALAT-1 was shuttled (LR clonase, Gateway technology, Invitrogen GmbH) into PINCO vector, a retroviral expression vector with puromycin resistance[26] and enhanced green fluorescent protein expression. Viral supernatants, supplemented with 5 μg/ml polybrene, were collected after 24, 48, and 72 hours. NIH 3T3 cells were transduced with PINCO vector supernatants.

Design and Cloning of Short Hairpin RNA Constructs

Four short hairpin RNA (shRNA) sequences (I, II, III, and IV) of MALAT-1 (Table 1) were designed using the DSIR Web site (Designer of Small Interfering RNA, http://biodev.extra.cea.fr/DSIR/DSIR.html). Specificity of the shRNA sequences was verified by BLAST search. A nonrelated 21 nt sequence was used as a negative shRNA control ("scrambed shRNA," Table 1). For shRNA expression, pRNAT-H1.1/Neo (Genscript Corp company, Piscataway, NJ) was used. Stable transfection of the cloned construct into A549 cell line was performed with Nanofectine reagent (PAA Laboratories GmbH, Cölbe, Germany) and cells were selected with Neomycin (G418, 1 mg/ml; Sigma-Aldrich Chemie GmbH, Munich, Germany). Cells were also transfected with a "pooled" shRNA, consisting of the shRNA II, III, and IV. MALAT-1 RNA expression levels were determined by quantitative real-time reverse transcription PCR.

Quantitative mRNA Analysis

For real-time PCR analysis, RNA was isolated with Qiagen RNeasy Micro Kit (Qiagen, Hilden, Germany). A total of 1 μg RNA from each sample was reverse-transcribed using random hexamer primer and Moloney murine leukemia virus reverse transcription (M-MLV RT; Invitrogen GmbH), according to the enzyme manufacturer's guidelines. Negative control reverse transcription samples were included without addition of M-MLV RT. SYBR-Green PCR master mix (Applied Biosystems Deutschland GmbH, Darmstadt, Germany) containing 333 nM of each forward (F) and reverse (R) primer (Table 1) and 2.5 μL reverse-transcribed template were transferred into a 96-well PCR plate (ABgene Germany, Hamburg, Germany). The primer used were as follows: human MALAT-1 (NR_002819) forward (5′-AAAGCAAGGTCTCCCCACAAG), human MALAT-1 reverse (5′-GGTCTGTGCTAGATCAAAAGGCA), murine

TABLE 1. Oligonucleotides for shRNA Constructions

shRNA	Starting Position	Nucleotide Sequence
I	166	GAGTTGTGCTGCTATCTTA
		TAAGATAGCAGCACAACTC
II	2087	GGAAGATAGAAACAAGATA
		TATCTTGTTTCTATCTTCC
III	6427	GGCTCTTCCTTCTGTTCTA
		TAGAACAGAAGGAAGAGCC
IV	8060	GAAATAACATGTTCAAGAA
		TTCTTGAACATGTTATTTC
Scrambled	Randomly	AGATCCGTATAGTGTACCTTA
		TAAGGTACACTATACGGATCT
Pooled	2087	shRNA II, III, IV
	6427	
	8060	

MALAT-1 (NR_002847) forward (5′-GTAGGTTAAGTTG ACGGCCGTTA), and murine MALAT-1 reverse (5′-ATC TTCCCTGTTTCCAACTCATG). PCR was performed in the Applied Biosystems 7500 Fast Real-Time PCR System (Applied Biosystems Deutschland GmbH). Melting curve analysis was used to monitor specificity of the PCR products. The PCR for each sample was performed in duplicate. Negative controls were always included. GAPDH mRNA was used as an internal control.

Immunofluorescence Microscopy

Transfected A549 cells and NIH 3T3 cells were grown on cover slips overnight in six-well plates. After fixation in 4% paraformaldehyde at 21°C for 20 minutes, cells were permeabilized with 0.2% Triton X-100, blocked in 10% goat serum, and incubated with 4′,6-diamidino-2-phenylindole (1: 3000; Invitrogen GmbH) and Alexa Fluor 594 phalloidin (1:100; Invitrogen GmbH). After consecutive washing steps with phosphate-buffered saline and distilled deionized water, mounting with Crystal Mount Medium (Sigma-Aldrich Chemie GmbH) was performed. For evaluation, an Axiovert 135 microscope with ApoTome equipment for epifluorescence (Carl Zeiss MicroImaging GmbH, Jena, Germany) was used.

Migration Assay

A total of 5×10^5 A549 cells (in 100 μL DMEM with 5% FCS) were seeded into the upper part of a transwell chamber (Transwell filter inserts in 6.5 mm diameter with a pore size of 5 μm; Corning Incorporated, Corning, NY), which was precoated with 50 μg/ml fibronectin for 30 minutes. In the lower part of the chamber, 600 μL DMEM with 20% FCS was added and the assay was performed for 16 hours at 37°C and 5% CO_2. Migrated cells were analyzed by flow cytometry. All assays were performed in triplicate and independently performed three times.

Soft Agar Colony Formation Assay

A total of 2×10^3 transfected A549 cells were added to 3 ml medium Iscove's Modified Dulbecco's Medium (IMDM; Invitrogen GmbH) + 10% FCS + 0.33% BD Difco Agar (Beckton Dickinson GmbH, Heidelberg, Germany), seeded on 35-mm tissue culture dishes and cultured at 37°C, high humidity, and 5% CO_2. Colonies were counted after 21 days growth by two investigators (J.H. and L.H.S.).

Cell Proliferation Assay

Transfected A549 cells (DMEM) were cultured at a density of 5×10^3 cells per well in a flat bottomed 96-well plate. cellTiter 96 (Promega Corporation, Madison, WI) was added to each well according to the manufacturer's instructions. Cell viability was determined by measuring the absorbance at 490 nm using a 550 BioRad plate-reader (Bio-Rad, Hertfordshire, UK) every 24 hours. All assays were performed in triplicate and independently repeated twice. As a blank control, 100 μL DMEM was used.

Tumor Mouse Model

Mice were housed and maintained in laminar airflow cabinets under specific pathogen-free conditions. A549 cells were harvested from culture flasks and transferred to serum-free PBS (PAA Laboratories GmbH). Single-cell suspensions (2×10^6 in 100 μL) were injected subcutaneously into the neck, left, and right shoulder of female CD1 nude mice (9–12 weeks old) obtained from Charles-River (Charles-River Laboratories, Sulzbach, Germany). Tumor size was evaluated using a standard caliper measuring tumor length and width in a blinded fashion and the tumor volume was calculated using the formula: length $\times$ width^2 $\times$ 0.52. After 31 days, animals were killed by cervical dislocation in deep CO_2 anesthesia, primary tumors were surgically removed, tumor weight (g) was determined, and expression levels of both human and murine MALAT-1 in the tumors were evaluated. Moreover, lungs, lymph nodes (axillary, inguinal), and adrenal glands were removed, photographed, and then frozen in liquid nitrogen or fixed in 4% formalin and paraffin embedded. For histological analyses, hematoxylin and eosin staining was performed. Immunohistochemical staining was performed using an antibody cytokeratin (monoclonal mouse anti-human cytokeratin, Clone MNF116, Isotype: IgG1, kappa, 1:300; Dako Deutschland GmbH, Hamburg, Germany). All experimental protocols were reviewed and approved by the Committee on Animal Experimentation.

Human NSCLC Samples for In Situ Hybridization (ISH) and RNA Analysis

Paraffin-embedded tissue microarray probes from 352 NSCLC patients (65 $\pm$ 9 years, 80% male, stage I-III) diagnosed and resected in the Department of Thoracic Surgery in Ostercappeln (Germany) between 1998 and 2005 were hybridized with MALAT-1 DNA probe. Clinical TNM staging (including clinical examination, CT scans, sonography, endoscopy, MRI, bone scan) was performed according to UICC/AJCC recommendations. To determine a definite tumor stage,[27,28] the postsurgical pathological examination was applied. Only patients with complete follow-up data and R_0 resected tumors were included in the statistical analysis ($n = 222$; mean 65 $\pm$ 8 years, 80% male, stage I–III). Besides, carcinoid tumors and unspecified NSCLC were excluded. According to the WHO classification of lung tumors,[29] the primary pulmonary lesion was classified as 102 squamous cell carcinomas (46%), 82 adenocarcinomas (37%), and 38 large cell carcinomas (17%). Overall survival (OS) time was calculated from the date of histological diagnosis to death, progressive disease, or last contact, respectively (Table 2).

Digoxigenin(DIG)-labeled DNA probes complementary to MALAT-1 RNA were generated using random prime labeling (Roche Diagnostics GmbH). For in situ hybridization, 5-μm-thick paraffin-embedded tissue microarrays were melted, dewaxed in xylene, rehydrated with 100% ethanol followed by 3% H_2O_2, and then incubated in pretreatment buffer at 95°C for 15 minutes. ZytoFast PLUS CISH Implementation Kit HRP-DAB (ZytoVision GmbH, Bremerhaven, Germany) was used for the detection of DIG-labeled ZytoFast CISH probes. Hybridization was performed overnight at 37°C. Duplex formation of the DIG-labeled probe was visualized using a primary (unmarked) anti-DIG antibody, detected by a secondary polymerized enzyme-conjugated antibody and the enzymatic reaction of DAB (3,3′-diaminobenzidine). For evaluation, the BX 51 microscope (Olympus)

TABLE 2. Baseline Characteristics of the Study Population ($n = 222$)

Parameter	$n = 222$	%[a]
Age[b] (yr)	65 ± 8	
Sex	178 males	80
Never smoker	46	21
Performance status		
ECOG—0	27	12
ECOG—I	186	84
ECOG—II	9	4
pT		
pT_1	65	29
pT_2	137	62
pT_{3+4}	20	9
pN		
pN_0	140	63
pN_{1-3}	82	37
pStage		
pStage I	130	59
pStage II	54	24
pStage III	38	17
Histological tumor type		
Squamous cell carcinoma	102	46
Adenocarcinoma	82	36
Large cell carcinoma	38	17
MALAT-1 transcript amplification		
Strong transcript amplification	83	37
OS time, days[c]	1163 (527, 1693)	

[a] Percent of nonmissing values.
[b] Mean ± SD.
[c] Median and quartiles (Q1, Q3).
ECOG, Eastern Cooperative Oncology Group; OS, overall survival.

was applied, equipped with ×40 and ×60 dry objectives and using 10 × 22 wide-field oculars. The microscope was connected to a digital imaging system. Immunoreactivity was interpreted and classified blindly by two investigators (L.H.S. and T.S.) according to Tanner et al,[30] where strong expression of MALAT-1 RNA was defined when a large gene copy cluster in 50% of carcinoma cells or numerous separate gene copies were seen. A weaker or absent expression of MALAT-1 RNA transcript was referred to as "weak expression."

To identify a human lung cancer that may have low endogenous MALAT-1 expression, we screened human nonsmall cell lung carcinoma tissues that were fresh frozen in the operation theater ($n = 10$). In the described cohort of 352 NSCLC patients, fresh frozen tissue was available from a minor percentage of patients only. Samples were randomly selected. With the help of an expert pathologist, only sections containing 100% tumor tissue were used for RNA extraction. Reverse-transcriptase (RT)-PCR analysis was performed in triplicates as described above.

Gene Expression Analyses

RNA was isolated from murine fibroblasts (NIH 3T3) either transduced with PINCO::MALAT-1 expression vector or with empty control vector. Technically, RNeasy Mini Kit (QIAgen, Hilden) and FastTrack 2.0 mRNA Isolation Kit (Invitrogen, Karlsruhe) were applied. RNA quality control was performed, using Agilent 2100 Bioanalyzer and RNA Labchip (Agilent Technologies, Santa Clara, CA). For gene expression profiling, the Mouse Gene 1.0 ST array (Affymetrix, Santa Clara, CA) was used. Each gene (in total $n = 28853$ genes) was represented by approximately $n = 27$ probes spread across the full length of the genes. Gene chips were prepared according to Affymetrix protocols (Affymetrix). In brief, after first- and second-strand synthesis and biotin labeling, the samples were hybridized onto the arrays for 16 hours at 45°C, rotating at 60 rpm. After washing (GeneChip FS-450 fluidics station; Affymetrix), the intensities were collected by scanning the arrays with GeneChip Scanner 3000 7G (Affymetrix).

The quality of the collected raw data was first analyzed with Affymetrix Expression Console software. After normalization (robust multichip average), log2 transformation, and annotation of the data, differential gene expression levels between the PINCO::MALAT-1 cells and the PINCO::empty control vector were evaluated using BRB array tools version 4.2.0 Beta 1. We identified 250 genes, which showed a twofold up-regulation or down-regulation. Consecutively, biological functions and network affiliations of these genes were evaluated with Ingenuity Pathways Knowledge Base (Ingenuity Pathways Analysis 9.0–3211 (Ingenuity Systems, http://www.ingenuity.com).

Statistical Analysis

All data were presented as means ± SEM if not indicated otherwise. The mean values of two groups were compared by Student's t test. Differences between multiple groups were analyzed by one-way ANOVA analysis. Survival curves were compared with the log-rank test. Univariate Cox survival analyses were performed and multivariate analyses were performed with the Cox proportional hazards. Features considered as potential explanatory factors were as follows (reference category in italics): sex (male versus female), age (<70 years versus ≥ 70 years), stage (I versus II and III), histological tumor type (squamous cell carcinoma versus nonsquamous cell carcinoma), and MALAT-1 expression (weak MALAT-1 expression versus strong MALAT-1 expression). To analyze the prognostic value of the potential explanatory factors for OS, a Cox proportional hazards model was applied using a forward stepwise selection (inclusion criteria: p value of the score test ≤0.05, exclusion criterion: p value of the likelihood ratio test > 0.1). $p < 0.05$ was considered significant for all tests. For all gene expression analyses, Benjamini-Hochberg multiple testing correction p values were used (log[B-H multiple testing correction p value]). For statistical analysis, SPSS 18 software (SPSS GmbH, München, Germany) was applied.

RESULTS

MALAT-1 Transcript in Human Lung Cancer

Previously, we identified MALAT-1 as a large ncRNA highly expressed in early-stage metastasizing NSCLC tumors[17] (Figure 1*A*). We now analyzed its biological functions. MALAT-1 transcript levels were evaluated in established hu-

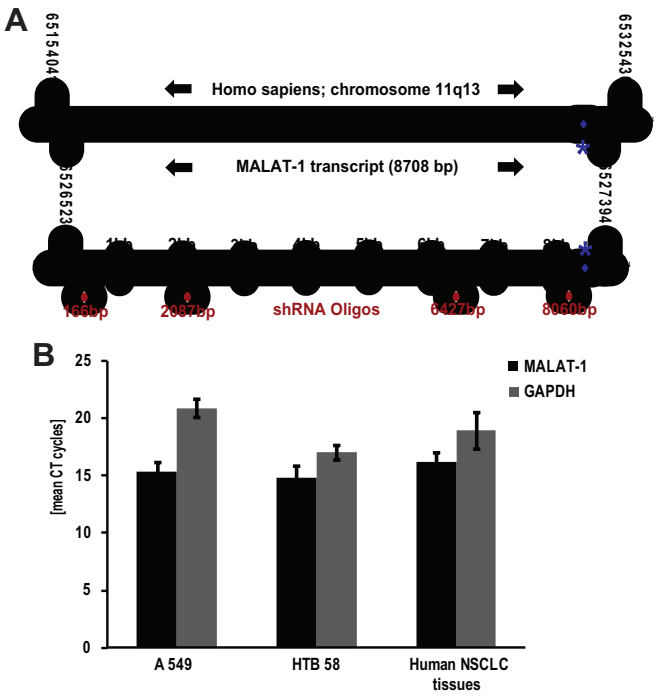

FIGURE 1. MALAT-1 transcript in human lung cancer. *A*, MALAT-1 transcript (8.7 kb) is located on chromosome 11q13, known for its strong impact on tumorigenesis and metastasis. To investigate the biological effect of MALAT-1, down-regulation was performed by four short hairpin RNA (shRNA) sequences at four positions (shRNA oligos—red color). A 61-nt RNA, referred to *mascRNA (*MALAT-1-associated small cytoplasmic RNA—blue color), reaches the cytoplasm.[11] *B*, According to quantitative RNA analysis, established human NSCLC cell lines A549, HTB 58, and NSCLC tissues (surgical resected specimens from 10 individuals) express high levels of MALAT-1 transcript if compared with human GAPDH (housekeeping gene). All columns, mean of three independent experiments performed in triplicate; bars, SD.

man NSCLC cell lines (A549, HTB 58) and fresh frozen human NSCLC tissue samples by quantitative RT-PCR analysis. For the tested cell lines and human NSCLC probes, MALAT-1 expression levels were very high with the transcript being detectable even earlier than the housekeeping gene human GAPDH (Figure 1*B*). This finding was reproducible with different amplicons (data not shown). Similar expression profiles for MALAT-1 and GAPDH were found in many other human malignant cell lines ($n = 3$ solid tumor cell lines [lung, cervix]; $n = 6$ leukemia cell lines, data not shown), confirming a high, robust MALAT-1 expression in malignancy.

MALAT-1 Expression Increases the Migratory Potential of Mouse Fibroblast Cells

To study the biological effects of increased MALAT-1 levels in nonmalignant cells, the entire MALAT-1 DNA was cloned and shuttled into a PINCO expression vector. Mouse fibroblast NIH 3T3 cells were transduced either with PINCO expression vector or with empty vector as negative control. As expected, transduction with PINCO expression vector resulted in high human MALAT-1 expression (Figure 2*A*). Interestingly, we also detected decreased murine MALAT-1 levels after human MALAT-1 transcript was transduced into NIH 3T3 cells (Figure 2*B*). The decrease of murine MALAT-1 indicated negative feedback regulation and a tight control of endogenous levels in nontransfected cells. Functionally, MALAT-1 transduction of NIH 3T3 cells increased transwell migration toward a high serum gradient compared with cells transduced with empty vector ($p = 0.001$, *t* test; Figure 2*C*).

Transduction of NIH 3T3 cells with MALAT-1 vector versus empty vector did not alter cell proliferation (MTS cell proliferation assay; data not shown). Neither could we observe morphological differences of nuclear or cytoplasmatic structures after counterstaining NIH 3T3 cells (transduced with either MALAT-1 vector or empty vector) with 4′,6-diamidino-2-phenylindole and phalloidin (data not shown).

Down-Regulation of MALAT-1 Expression Reduces Migration Potential

Because we demonstrated human MALAT-1 transcript to increase migration potential in mouse fibroblast cell line NIH 3T3, we next studied the biological effects of MALAT-1 down-regulation. Because of its high MALAT-1 expression levels, the A549 cell line was selected to analyze the effects of down-regulation. Four shRNA oligos against MALAT-1 were constructed (Table 2) and cloned into pRNAT-H1.1/Neo vector. Next, human A549 NSCLCs were transfected with pRNAT-H1.1/Neo vector, expressing shRNA against MALAT-1. As a control, A549 cells were also transfected with "scrambled" control shRNA, without effect on MALAT-1 expression. Transfected cells were sorted for GFP positivity by flow cytometry (data not shown).

RT-PCR analysis demonstrated decreased MALAT-1 expression after transfection of A549 cells with shRNA expressing pRNAT-H1.1/Neo vector. Strongest down-regulation was achieved when a combination of three shRNA (II, III, and IV; Table 2) was transfected (Figure 3*A*). Functionally, migration array revealed less migration toward a serum gradient of A549 cells either transfected with shRNA "III" ($p < 0.001$, *t* test) or "pooled" shRNA (II, III, and IV; $p < 0.001$, *t* test), compared with "scrambled" control shRNA (Figure 3*B*). Similarly, soft agar colony formation assay demonstrated fewer colonies per well after 21 days for A549 cells transfected with pooled shRNA (II, III, and IV) versus "scrambled" control shRNA ($p < 0.001$, *t* test, Figure 3*C*).

Similar to NIH 3T3, no morphological differences between A549 cells transfected with "pooled" shRNA and "scrambled" control shRNA were seen after counterstaining with 4′,6-diamidino-2-phenylindole and phalloidin (data not shown). Also, no altered growth properties or direct proliferative advantages were observed in vitro (MTS cell proliferation assay; data not shown).

Down-Regulation of MALAT-1 Expression Reduces Tumor Growth In Vivo

A549 cells transfected with either "scrambled" control shRNA or "pooled" shRNA (II, III, IV) were subcutaneously injected into nude mice ($n = 10$). Tumor growth was monitored by standard caliper measuring in a blinded fashion.

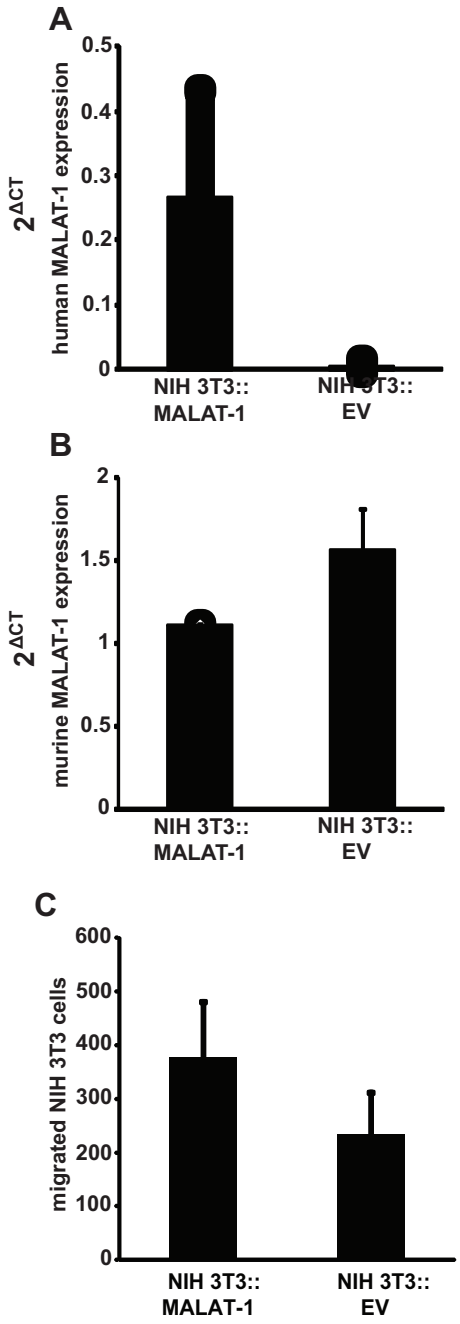

FIGURE 2. Transduction of MALAT-1 into NIH 3T3 cells increases the migratory potential. *A*, NIH 3T3 cells were transduced with MALAT-1 expression PINCO vector. MALAT-1 expression analysis by RT-PCR analysis revealed high expression of human MALAT-1 transcript in MALAT-1 transduced NIH 3T3 cells compared with control (NIH 3T3 cells transduced with empty vector, EV). *B*, On MALAT-1 transduction, NIH 3T3 cells showed reduced expression of murine MALAT-1 compared with EV transduced NIH 3T3 cells. *C*, Expression of human MALAT-1 transcript in NIH 3T3 cells was associated with increased migration potential (migration assay; $p = 0.001$, *t* test). All bars indicate the mean of three independent experiments performed in triplicate; bars, SD.

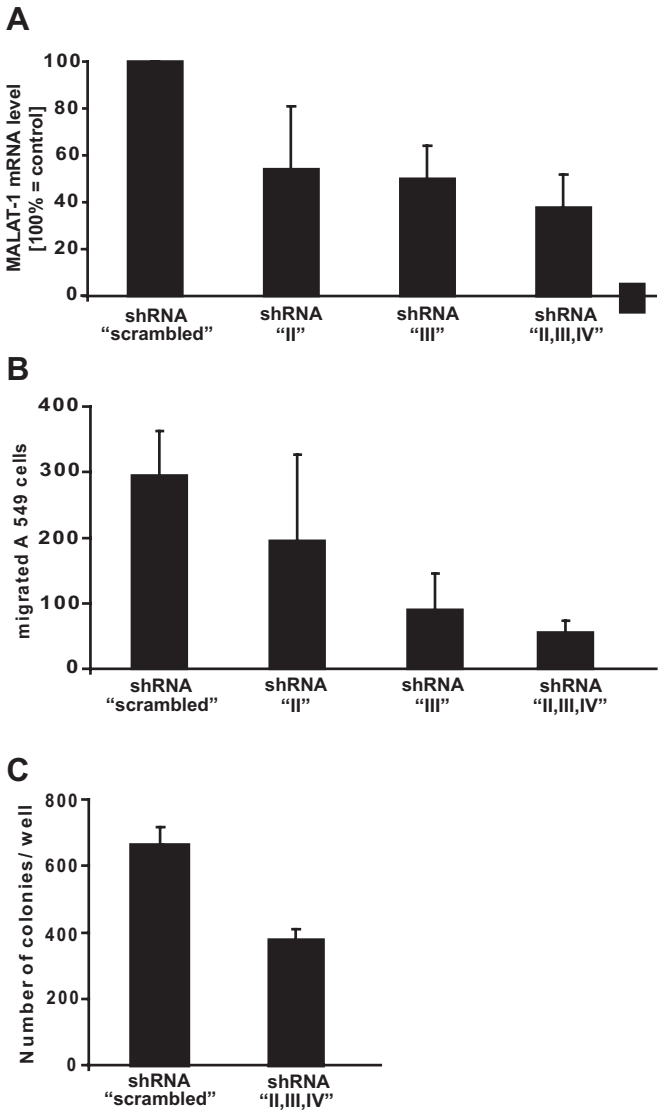

FIGURE 3. Down-regulation of MALAT-1 expression in human A549 NSCLCs reduced migration. *A*, After transfection of A549 cells with shRNA (II; III; II, III, IV) against MALAT-1, expression of MALAT-1 is decreased, as demonstrated by reverse-transcriptase polymerase chain reaction (RT-PCR) analysis. Most effective down-regulation is achieved, if three shRNA (II, III, IV) are transfected at once in A549 cell. *B*, Significantly reduced transwell migration of A549 cells transfected with shRNA against MALAT-1 was found if either shRNA "III" ($p < 0.001$, *t* test) or "pooled" shRNA (II,III,IV; $p < 0.001$, *t* test) was used, compared with "scrambled." *C*, Soft agar colony formation assay showed less colonies per well after 21 days growth of A549 cells transfected with three shRNA (II, III, IV), if compared with A549 cells ($p < 0.001$, *t* test control versus II, III, IV). All columns, mean of three independent experiments performed in triplicate; bars, SD.

After 31 days, animals were killed for determination of tumor weights and immunohistochemistry.

As shown in Figure 4*A*, tumor development was first visible 7 days after injection. Tumors of A549 cells transfected

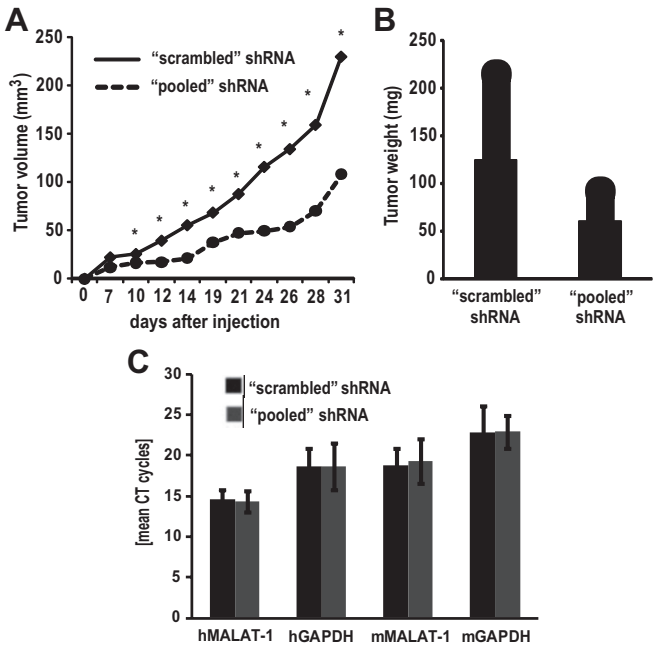

FIGURE 4. MALAT-1 gene knockdown suppresses tumor growth and metastasis in nude mice. *A*, A549 cells transfected with either scrambled control or pooled shRNA (II, III, IV) were injected subcutaneously into nude mice (n = 10) at three locations each. After 31 days, animals were killed for determination of tumor weights and immunohistochemistry. Injected cells transfected with shRNA against MALAT-1 demonstrated reduced tumor growth (volume) when compared with scrambled-transfected cells (*$p < 0.05$). *B*, According to tumor volume, tumor weight was significantly less in the "pooled" shRNA group compared with the "scrambled" shRNA group ($p = 0.021$). *C*, On day 31, murine MALAT-1 (mMALAT-1), human MALAT-1 (hMALAT-1), murine GAPDH (mGAPDH), and human GAPDH (hGAPDH) gene expression, respectively, were evaluated using RT-PCR. In all test sets, no difference between both tumor types (A 549 scrambled shRNA versus A 549 pooled shRNA) were found.

with "pooled" shRNA (II, III, IV) grew significantly slower (volume) in comparison with tumors of A549 cells transfected with "scrambled" control shRNA (*$p < 0.05$, *t* test, Figure 4*A*). In addition, tumor weight at the time of resection was also reduced ($p = 0.021$, *t* test, Figure 4*B*). Nevertheless, quantitative MALAT-1 and GAPDH transcript expression in the tumors derived from treated A549 cell line and from the untreated control cell line did not differ (Figure 4*C*).

Both histological and immunohistochemical analysis with cytokeratin antibody confirmed tumor histology of the transplanted cell grafts (data not shown). These observations suggest that MALAT-1 promotes tumor growth in vivo. Actually, this mouse model was used to study tumor growth, and although it is not an established metastasis model, we discovered one tumor metastasis in a left axillary lymph node of one mouse, which received A549 cells transfected with "scrambled" control shRNA. Besides, no other metastasis could be found on examination of the other lymph nodes (axillary, inguinal), adrenal glands, or lungs.

Prognostic Role of MALAT-1 Expression

In situ hybridization was used to investigate MALAT-1 expression in a large cohort of paraffin-embedded tumor tissue samples of NSCLC patients (Table 2). The MALAT-1 transcript was predominantly localized in nuclei of tumor cells, whereas the cytoplasm did not show specific signals (Figure 5*C*). In nonmalignant normal lung tissue, MALAT-1 transcript was barely detectable (Figure 5*D*). In total, strong MALAT-1 transcript expression was observed in 123 (35%) of the tested 352 NSCLC tissues (Table 2).

For clinicopathological correlations, Fisher's exact test revealed significant associations of strong MALAT-1 expression both with adenocarcinoma ($p = 0.004$) and large cell carcinoma ($p = 0.027$). All the other variables including sex, age, smoker, tumor size, lymph node status, tumor stage, and squamous cell carcinoma did not show any significant association with strong MALAT-1 expression (data not shown).

To evaluate survival, univariate log-rank test was performed independently for squamous and nonsquamous tumor histology. For squamous cell carcinoma, strong MALAT-1 expression was shown to be associated with poor prognosis ($p = 0.012$; log-rank test; Figure 5*E*), whereas for nonsquamous cell carcinoma positive MALAT-1 expression did not show a significant effect on prognosis ($p = 0.108$; log-rank test; data not shown).

The prognostic effect of MALAT-1 was also confirmed in forward likelihood selection model using Cox proportional hazards. NSCLC patients with squamous cell carcinoma, whose tumors displayed a strong hybridization signal, showed a worse outcome (OS hazard ratio = 1.78; 95% CI = 1.084–2.922; $p = 0.026$). Stage was the second explanatory factor. In contrast, in NSCLC patients with nonsquamous cell carcinoma, histology stage and age showed a prognostic impact on OS but not MALAT-1 expression (Table 3).

Gene Expression Analyses

The results of the gene expression analysis of 250 selected genes were categorized into three "Top Bio Functions" groups. Among the group "Diseases and Disorders," the two highest ranking items were "cancer" with 113/250 molecules (log[B-H *p* value]: 1.6E-11–4.2E-04) and "inflammatory response" ($n = 65$; 3.9E-12–4.8E-04). Similarly, the "Molecular and Cellular Functions" group had the most hits for "Cellular Growth and Proliferation" ($n = 90$; 7E-10–4.6E-04) and "Cellular movement ($n = 75$; 9.5E-14–4.8E-04). Within the third group, "Physiological System Development and Function," "Hematological System Development and Function" ($n = 76$; 6.7E-09–4.5E-04), and "Tissue Development" ($n = 66$; 1E-08–3.5E-04) ranked highest. These results strongly confirm the reported functional effects of MALAT-1.

DISCUSSION

NSCLC ranks among the most common and lethal malignant diseases.[1] Poor prognosis of early stage NSCLC is crucially linked to the onset of tumor metastasis.[3] The processes inducing and stimulating metastasis are complex and still not well understood. In early-stage NSCLC that subsequently metastasized, we found the long noncoding RNA

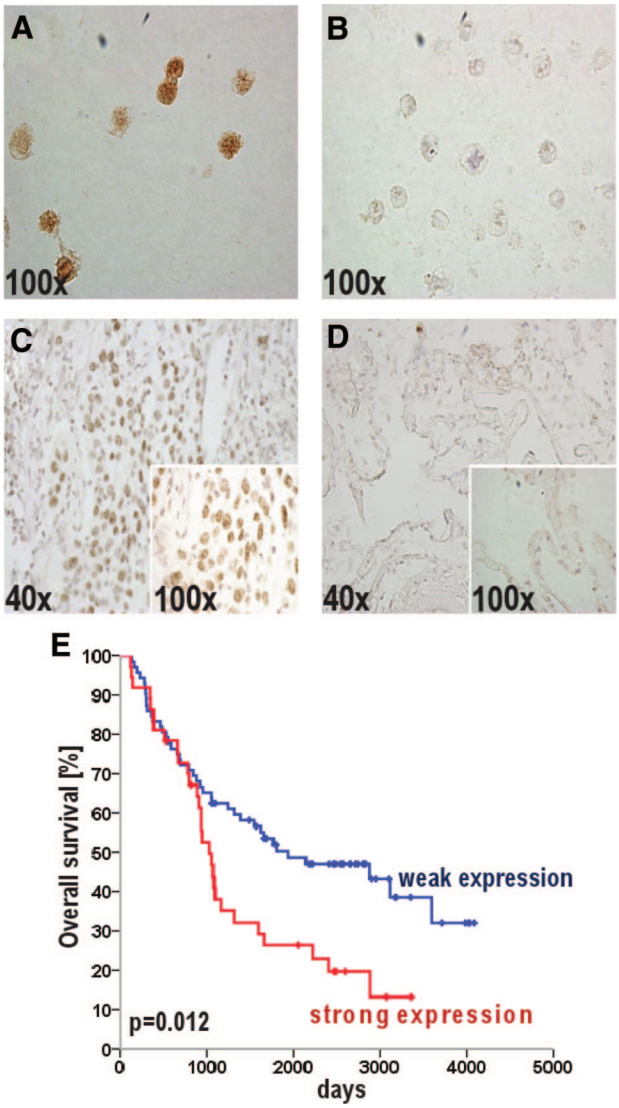

FIGURE 5. Prognostic role of MALAT-1 expression evaluated by chromogenic in situ hybridization. To evaluate the sensitivity of the ISH probe, hybridization was first tested in A549 cells. *A*, Strong hybridization signal of MALAT-1 RNA after transfection of A549 cells with "scrambled" control shRNA (pRNAT-H1.1/Neo vector). If A549 cells were transfected with "scrambled" control shRNA (pRNAT-H1.1/Neo vector), a strong amplification signal was detected. *B*, After transfection of "pooled" shRNA, MALAT-1 amplification signal was weak, indicating gene knock-down. *C*, Strong MALAT-1 transcript hybridization signals were observed in 123 (35%) of the tested 352 NSCLC tissues. Representative MALAT-1 staining is shown for squamous cell carcinoma (blue, hematoxylin counterstaining of nuclei). *D*, In contrast to NSCLC tissues, nonmalignant lung tissue showed a weak amplification signal of MALAT-1 RNA. *E*, Kaplan-Meier curves were used to determine the survival probability, and the log-rank test was used to compare the survival curves between patients with and without MALAT-1 hybridization signals. Blue indicates weak expression of MALAT-1 transcript and the red line stands for positive expression. For pulmonary squamous cell carcinoma, positive MALAT-1 expression indicated poor prognosis ($p = 0.012$; log-rank test).

TABLE 3. OS: Explanatory Prognostic Factors for OS Accepted in the Likelihood Forward Selection Model

OS Explanatory Factors[a]	Squamous Cell Carcinoma			Nonsquamous Cell Carcinoma		
	HR[b]	95% CI	p[c]	HR[b]	95% CI	p[c]
P stage[d]			0.016			<0.001
P stage II	1.72	1.00–2.98		2.10	1.24–3.58	
P stage III	2.45	1.30–4.62		3.60	1.95–4.66	
MALAT-1 expression[e]	1.78	1.08–2.92	0.026	—[f]		
Age ≥70 y[g]	—[f]			1.84	1.11–3.07	0.024

[a] Other factors not accepted by Cox regression model: sex (male [reference] vs. female) and smoking status (smoker and ex-smoker [reference] vs. nonsmoker).
[b] HR <1 suggests improved survival.
[c] p value according to the likelihood ratio test.
[d] Pathological TNM tumor stage, categorized as stages I, II, and III, respectively. P stage I is reference category.
[e] Expression corresponds to the intensity of ISH hybridization signal, categorized as weak (reference) vs. moderate/strong.
[f] Not accepted from forward selection model.
[g] Age was categorized as <70 yr (reference) vs. ≥70 yr.
OS, overall survival; HR, hazard ratio; CI, confidence interval.

(ncRNA) MALAT-1 at chromosome 11q13 to be overexpressed with potential impact on metastasis.[17] ncRNAs account for approximately the 1.5% of the transcriptional output of mammalian genomes.[31] Besides MALAT-1, other ncRNAs have also been described to be associated with tumorigenesis and patient prognosis (e.g., HULC in hepatocellular carcinoma[32]). MALAT-1 is predominantly localized in nuclear speckles.[16,33] By 3′ end processing, a 61-nt RNA is generated, which is transferred to the cytoplasm. This small RNA is called mascRNA (MALAT-1-associated small cytoplasmic RNA). Compared with nuclear MALAT-1 ncRNA, mascRNA is less stable. Because of its tRNA-like cloverleaf secondary structure and the fact that mascRNA cannot be aminoacylated imply an interfering effect on the tRNA processing machinery, possibly due to tRNA mimicry. It was also postulated that the mascRNA might regulate MALAT-1 levels.[11] In line with this hypothesis, our analyses in NIH 3T3 cells and NSCLC cell lines suggest that endogenous MALAT-1 levels are tightly regulated and that an effective feedback loop exists. These findings suggest that MALAT-1 plays an important functional role. Recently, one study demonstrated MALAT-1 to be negatively related with the dephosphorylated pool of serine/arginine splicing factors and thus to influence alternative splicing.[33]

In this study, we identified MALAT-1 as a strong regulator for NSCLC migration and invasion in vitro. The proliferative activity was not affected in vitro. In contrast, significantly impaired tumor growth was observed in vivo. This might indicate that the invasive phenotype associated with MALAT-1 expression might lead to faster tumor growth in vivo, while cell cycle regulation of individual tumor cells is not affected. Similarly, apoptosis was not affected by MALAT-1 suppression and at least a suppression of the RNA level by 75% was not sufficient to induce cell death.

Of great interest, gene expression analysis using the Affimetrix Gene Chip technology of the full length of 28853 mouse genes strongly confirmed the observed functional

effects of MALAT-1 in vitro and in vivo. Analyzing network affiliations of differentially expressed genes upon MALAT-1 up-regulation with Ingenuity Pathways Knowledge Base, MALAT-1 up-regulation is mostly associated with alterations of the signaling pathways of "cancer," "inflammatory response," "Cellular Growth and Proliferation," "Cellular movement," "Hematological System Development and Function," and "Tissue Development."

Although the applied mouse model is not an established metastasis model, we discovered one lymph node metastasis in one mouse, transplanted with A549 cells transfected with "scrambled" control shRNA. This finding might therefore indicate increased metastasis development of tumors with high MALAT-1 expression. The prognostic role of MALAT-1 was further corroborated in this study by in situ hybridization of a large collection of primary NSCLC tumors. Importantly, MALAT-1 was expressed across all tumor stages and subtypes. High MALAT-1 levels were found for squamous cell carcinomas and indicated decreased survival in patients with entirely resected NSCLC. The in situ hybridization results did not show (as in the real-time PCR study) that especially high expression levels of MALAT-1 also predicted survival in adenocarcinoma. However, in situ hybridization is much less sensitive and quantitative than real-time PCR. Nonetheless, this study along with previous results provides evidence that high MALAT-1 expression in NSCLC indicates a poor prognosis in patients suffering from squamous cell carcinoma of the lung. The biological function of MALAT-1 to stimulate migration, invasion, and tumor growth in vivo is thus in line with the clinical findings in NSCLC patients.

In conclusion, MALAT-1 is the first large coding RNA that regulates metastasis development in NSCLC and probably in other cancers that overexpress MALAT-1. These results indicate that MALAT-1 might be an important biomarker and a novel therapeutic target.

ACKNOWLEDGMENTS

Supported by the Innovative Medizinische Forschung Münster University (IMF: I-SC110818), Deutsche Krebshilfe e. V. (107888), and Wilhelm Sander-Stiftung *(2009.041.1).*

The authors thank Judith Obernüfemann, Beate Lindner, and Konstantin Agelopoulos for their technical assistance and helpful advice.

REFERENCES

1. Parkin DM, Bray F, Ferlay J, et al. Global cancer statistics, 2002. *CA Cancer J Clin* 2005;55:74–108.
2. Jemal A, Siegel R, Ward E, et al. Cancer statistics, 2007. *CA Cancer J Clin* 2007;57:43–66.
3. Fidler IJ. Critical factors in the biology of human cancer metastasis: twenty-eighth G.H.A. Clowes memorial award lecture. *Cancer Res* 1990;50:6130–6138.
4. Langley RR, Fidler IJ. Tumor cell-organ microenvironment interactions in the pathogenesis of cancer metastasis. *Endocr Rev* 2007;28:297–321.
5. Ji H, Ramsey MR, Hayes DN, et al. LKB1 modulates lung cancer differentiation and metastasis. *Nature* 2007;448:807–810.
6. Karnoub AE, Dash AB, Vo AP, et al. Mesenchymal stem cells within tumour stroma promote breast cancer metastasis. *Nature* 2007;449:557–563.
7. Nguyen DX, Massague J. Genetic determinants of cancer metastasis. *Nat Rev Genet* 2007;8:341–352.
8. Eddy SR. Non-coding RNA genes and the modern RNA world. *Nat Rev Genet* 2001;2:919–929.
9. Birney E, Stamatoyannopoulos JA, Dutta A, et al. Identification and analysis of functional elements in 1% of the human genome by the ENCODE pilot project. *Nature* 2007;447:799–816.
10. Kapranov P, Cheng J, Dike S, et al. RNA maps reveal new RNA classes and a possible function for pervasive transcription. *Science* 2007;316:1484–1488.
11. Wilusz JE, Freier SM, Spector DL. 3′ end processing of a long nuclear-retained noncoding RNA yields a tRNA-like cytoplasmic RNA. *Cell* 2008;135:919–932.
12. Calin GA, Croce CM. MicroRNA signatures in human cancers. *Nat Rev Cancer* 2006;6:857–866.
13. Costa FF. Non-coding RNAs: new players in eukaryotic biology. *Gene* 2005;357:83–94.
14. Bartels CL, Tsongalis GJ. MicroRNAs: novel biomarkers for human cancer. *Clin Chem* 2009;55:623–631.
15. Carthew RW, Sontheimer EJ. Origins and mechanisms of miRNAs and siRNAs. *Cell* 2009;136:642–655.
16. Hutchinson JN, Ensminger AW, Clemson CM, et al. A screen for nuclear transcripts identifies two linked noncoding RNAs associated with SC35 splicing domains. *BMC Genomics* 2007;8:39.
17. Ji P, Diederichs S, Wang W, et al. MALAT-1, a novel noncoding RNA, and thymosin beta4 predict metastasis and survival in early-stage non-small cell lung cancer. *Oncogene* 2003;22:8031–8041.
18. Bekri S, Adelaide J, Merscher S, et al. Detailed map of a region commonly amplified at 11q13–>q14 in human breast carcinoma. *Cytogenet Cell Genet* 1997;79:125–131.
19. Chakrabarti R, Srivatsan ES, Wood TF, et al. Deletion mapping of endocrine tumors localizes a second tumor suppressor gene on chromosome band 11q13. *Genes Chromosomes Cancer* 1998;22:130–137.
20. Lin R, Maeda S, Liu C, et al. A large noncoding RNA is a marker for murine hepatocellular carcinomas and a spectrum of human carcinomas. *Oncogene* 2007;26:851–858.
21. Tseng JJ, Hsieh YT, Hsu SL, et al. Metastasis associated lung adenocarcinoma transcript 1 is up-regulated in placenta previa increta/percreta and strongly associated with trophoblast-like cell invasion in vitro. *Mol Hum Reprod* 2009;15:725–731.
22. Lamond AI, Spector DL. Nuclear speckles: a model for nuclear organelles. *Nat Rev Mol Cell Biol* 2003;4:605–612.
23. Lieber M, Smith B, Szakal A, et al. A continuous tumor-cell line from a human lung carcinoma with properties of type II alveolar epithelial cells. *Int J Cancer* 1976;17:62–70.
24. Morita S, Kojima T, Kitamura T. Plat-E: an efficient and stable system for transient packaging of retroviruses. *Gene Ther* 2000;7:1063–1066.
25. Magnani E, Bartling L, Hake S. From Gateway to MultiSite Gateway in one recombination event. *BMC Mol Biol* 2006;7:46.
26. Grignani F, Kinsella T, Mencarelli A, et al. High-efficiency gene transfer and selection of human hematopoietic progenitor cells with a hybrid EBV/retroviral vector expressing the green fluorescence protein. *Cancer Res* 1998;58:14–19.
27. Mountain CF. Revisions in the International System for Staging Lung Cancer. *Chest* 1997;111:1710–1717.
28. Sobin LH, Fleming ID. TNM Classification of Malignant Tumors, fifth edition (1997). Union Internationale Contre le Cancer and the American Joint Committee on Cancer. *Cancer* 1997;80:1803–1804.
29. Travis WD, Colby TV, Corrin B, et al. Histological Typing of Lung and Pleural Tumours, 3rd Ed. Berlin, Heidelberg, New York: Springer Verlag Berlin Heidelberg, 1999.
30. Tanner M, Gancberg D, Di LA, et al. Chromogenic in situ hybridization: a practical alternative for fluorescence in situ hybridization to detect HER-2/neu oncogene amplification in archival breast cancer samples. *Am J Pathol* 2000;157:1467–1472.
31. Mattick JS, Makunin IV. Non-coding RNA. *Hum Mol Genet* 2006;15(Spec No 1):R17–R29.
32. Panzitt K, Tschernatsch MM, Guelly C, et al. Characterization of HULC, a novel gene with striking up-regulation in hepatocellular carcinoma, as noncoding RNA. *Gastroenterology* 2007;132:330–342.
33. Tripathi V, Ellis JD, Shen Z, et al. The nuclear-retained noncoding RNA MALAT1 regulates alternative splicing by modulating SR splicing factor phosphorylation. *Mol Cell* 2010;39:925–938.